

Supporting information

Novel properties of 0D metal-organic polyhedra bonded to the surfaces of 2D graphene and 1D single-walled carbon nanotubes

Ram Kumar and C. N. R. Rao

Experimental Section:

Reagents and Precursors: All the chemicals used in synthesis were of high purity and obtained from commercial sources. Graphite oxide (GO) was synthesized using the modified Hummers method.¹ Graphite oxide (GO) was placed in an alumina boat inside a quartz tube and inserted into the heating zone of tube furnace maintained at 1050 °C under constant N₂ flow to obtain the exfoliated graphene (EG). Purified CoMoCAT single-walled carbon nanotubes (SWNT) were used for the synthesis of composites. Carboxylate functionalized graphene and single-walled carbon nanotubes (SWNT) were prepared under microwave irradiation. In a typical batch, 100 mg graphene or SWNT was placed in 100 ml polytetrafluoroethylene (PTFE) microwave reactor, 4 ml conc. HNO₃, 4 ml conc. H₂SO₄ and 30 ml water were irradiated with microwave at 450 W for 10 min followed by heating in an oven at 100 °C for 12 h. Obtained product was filtered with 0.45 μm PTFE membrane, washed with copious amount of water to remove excess acid followed by washing with ethanol and dried under vacuum.

Hydroxylated metal-organic polyhedra (MOP): Hydroxylated metal-organic polyhedral were generated by the procedure by Li *et al.*² In a typical batch, 5-hydroxyisophthalic acid (365 mg) dissolved in 10 ml methanol (MeOH) was mixed with a MeOH solution (30 ml) of cupric acetate monohydrate (Cu₂(OAc)₄·2H₂O, 400 mg) and stirred for 30 min. Subsequently, 10 ml *N,N*-Dimethylacetamide (DMA) was added and allowed to stand at room temperature for 30 days. The product was filtered (0.45 μm, nylon) washed with DMA and acetone and dried under vacuum.

MOPGr composites: In a typical batch 40 mg carboxylated graphene was dispersed in 40 ml MeOH by probe sonication. In the homogeneous dispersion, X mg (X = 10 mg, 20 mg and 40 mg) of hydroxylated MOP dissolved in 5–7 ml MeOH was added drop wise and allowed to stir for 12 hours at room temperature. The solvent was evaporated at 40 °C under vacuum. The obtained MOPGr-X composites are designated as MOPGr-1, 2 and 3.

MOPNT composites: Two different MOPNT-X composites were obtained according to the procedure as for graphene composites. 20 mg carboxylated-SWNT was used and two different compositions MOPNT-1 and 2 ($X = 10$ mg and 20 mg MOP) were prepared.

Characterization: Powder X-ray diffraction (PXRD) pattern was recorded in Bruker diffractometer using Cu $K\alpha$ radiation. PXRD pattern of pristine MOP crystals were immediately collected after filtration from the mother liquor. FTIR spectra were recorded on a Perkin-Elmer spectrometer using attenuated-total-reflectance (ATR) accessories. Raman spectra were collected at several different spots in the back scattering geometry using a 514.5 nm Ar^+ laser with a HORIBA LabRam HR800 spectrometer. Elemental mapping using energy-dispersive X-ray spectroscopy (EDAX) and scanning electron microscope images were obtained using a Nova Nano SEM 600, FEI. Transmission Electron Microscope (TEM) images were collected with the FEI Tecnai instrument employing an accelerating voltage of 200 kV. Thermogravimetric analysis (TGA) was performed using a Mettler Toledo TGA 850 in the N_2 atmosphere at a heating rate of 3 $^{\circ}C/min$. The N_2 sorption isotherm at 77 K was obtained using QUANTACHROME QUADRASORB-SI analyzer. The samples were heated at 343 K under vacuum for 12 h prior to the measurement of the isotherm. NMR spectrum was recorded in a Bruker 400 MHz NMR spectrometer.

Catalytic tests: Catalytic reactions were performed in a Schlenk flask with the CO_2 cylinder connected to the Schlenk line. Prior to the reaction, the catalysts were activated at 50 $^{\circ}C$ under vacuum for 12 h. In a typical batch, catalyst (0.03 mol% calculated based on copper paddlewheel units) and co-catalyst tetra-*n*-butylammonium bromide (TBAB, 3 mmol) were sealed in a Schlenk flask with a rubber septum, evacuated under vacuum and purged with CO_2 for 3 cycles. Propylene oxide (100 mmol) was added to the reaction mixture and allowed to stir for 48 h at room temperature with CO_2 purging. The reaction mixture was centrifuged to separate the catalyst, washed with $CHCl_3$ and activated at 50 $^{\circ}C$ under vacuum before next run. The product was evacuated under vacuum to remove any unreacted propylene oxide. The obtained product was analyzed by a gas chromatograph-mass spectrometer (Shimadzu GCMS-QP2010 plus fitted with MS detector) and yields were determined. The same weights of carboxylated graphene and SWNT were used in the control reaction as the main catalysts. The reaction product of MOPGr catalyst was further distilled under vacuum at 180 $^{\circ}C$ to obtain purified propylene carbonate.

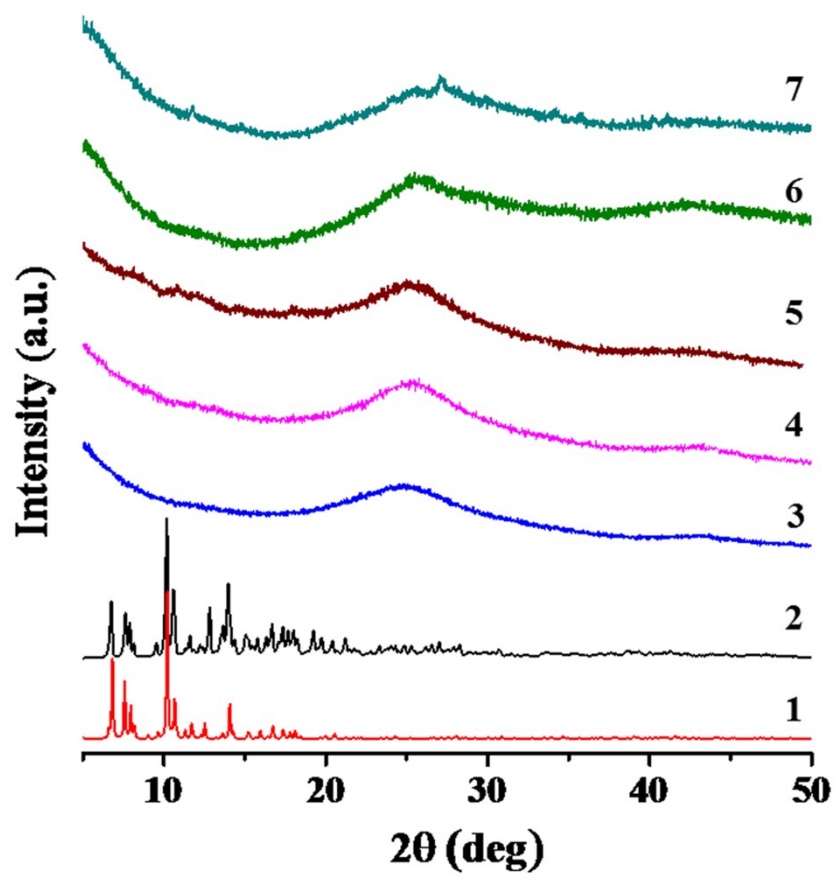


Fig. S1 (1) Calculated powder X-ray diffraction (PXRD) pattern of MOP. Powder X-ray diffraction patterns of (2) pristine-MOP, (3) MOPGr-1, (4) MOPGr-2, (5) MOPGr-3, (6) MOPNT-1 and (7) MOPNT-2.

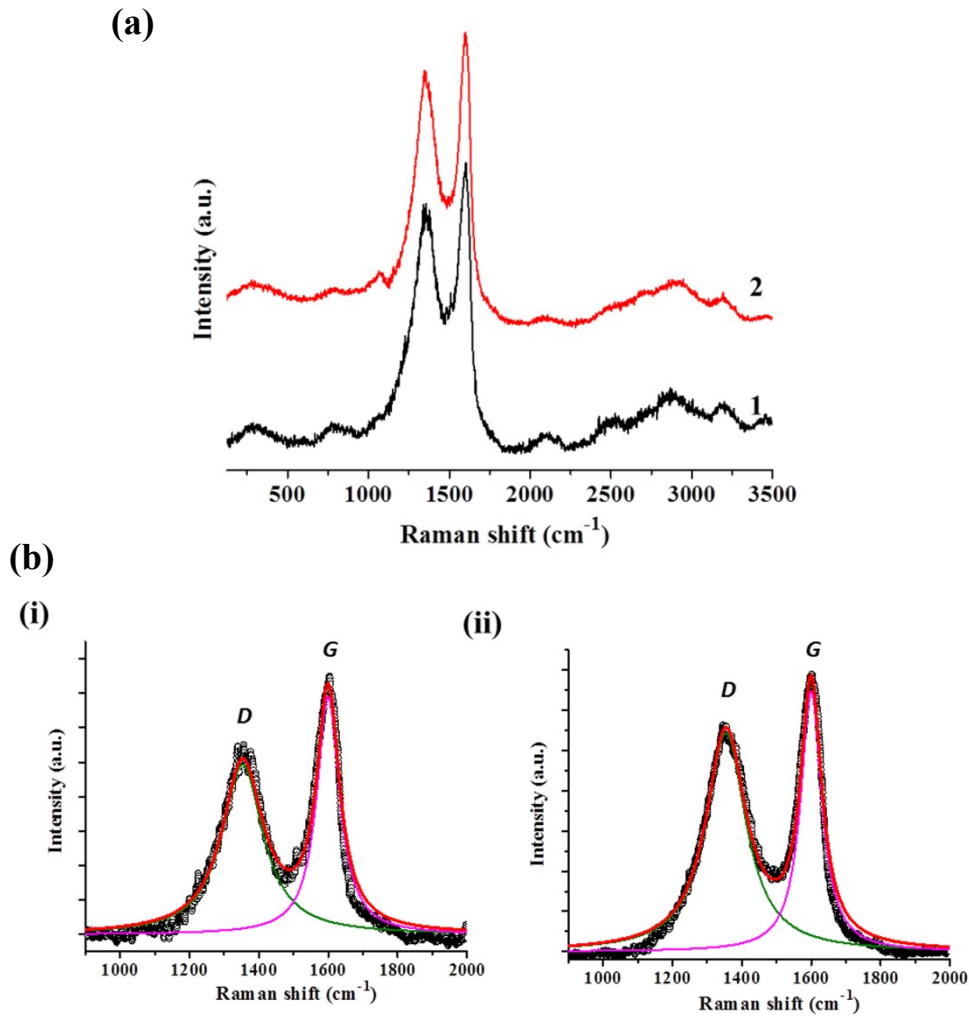


Fig. S2 (a) Raman spectra of (1) exfoliated-graphene (EG) and (2) carboxylated-graphene. (b) Raman spectra of (i) exfoliated-graphene and (ii) carboxylated-graphene fitted to Lorentzian line shape showing an enhancement in I_D/I_G ratio due to carboxylic acid functionalization.

Table S1: Peak parameters of exfoliated graphene and carboxylated graphene fitted to Lorentzian line shape.

Entry	Sample name	Peak assignment (band)	Peak position (cm ⁻¹)	FWHM (cm ⁻¹)	Line shape	Peak Area*	Intensity ratio (I_D/I_G)
1.	Exfoliated-graphene	<i>D</i>	1354	144	Lorentzian	22230	1.28
2.	Exfoliated-graphene	<i>G</i>	1600	80	Lorentzian	17340	1.28.
3.	Carboxylated-graphene	<i>D</i>	1357	140	Lorentzian	60542	1.6
4.	Carboxylated-graphene	<i>G</i>	1600	74	Lorentzian	37510	1.6

*Since we are interested in calculating I_D/I_G ratio and intensity axis is arbitrary unit, no unit is mentioned for the area.

The graphene sample has been prepared by thermal exfoliation of graphite oxide. Due to the use of graphite oxide as starting precursor, the sample has a high defect, and hence I_D/I_G ratio of 1.28 is observed for exfoliated graphene. Further, a weak G' (around 2700 cm^{-1}) band merging with $D + G$ band at 2955 cm^{-1} is observed due to defects on the graphene basal plane.³ The carboxylic acid functionalization increases the density of sp^3 centers on graphene basal plane and I_D/I_G ratio increase to 1.6. The defect centers present on exfoliated graphene basal plane helps in functionalization provides additional adsorbate accessible space and increases the catalytic activity.

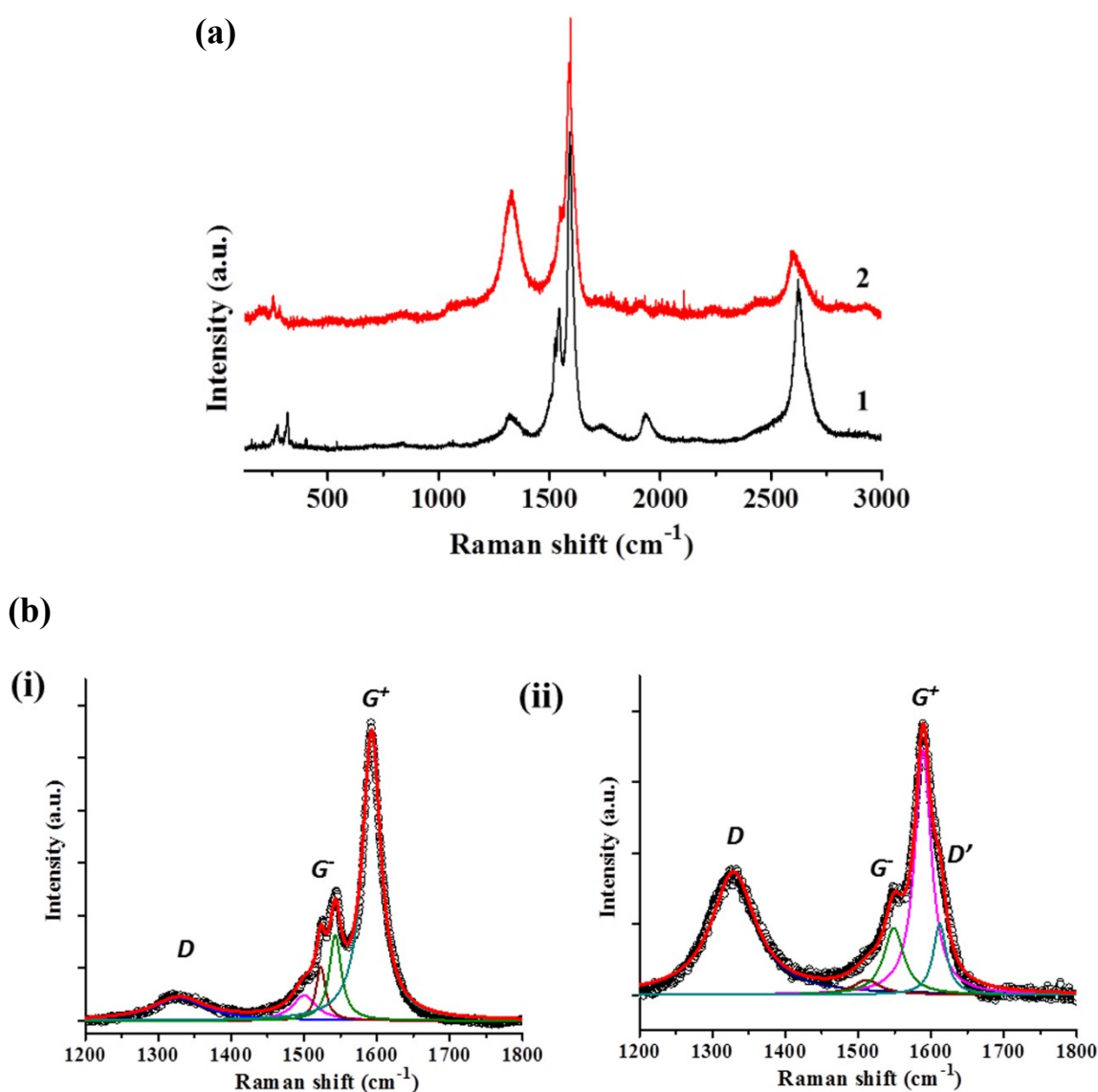


Fig. S3 (a) Raman spectra of (1) single-walled carbon nanotube (SWNT) and (2) carboxylated-SWNT. (b) Raman spectra of (i) SWNT and (ii) carboxylated-SWNT fitted to Lorentzian line shape showing an enhancement in I_D/I_G ratio due to carboxylate functionalization.

Table S2: Peak parameters of single-walled carbon nanotubes (SWNTs) and carboxylated-SWNTs fitted to Lorentzian line shape.

Entry	Sample name	Peak assignment(band)	Peak position (cm ⁻¹)	FWHM (cm ⁻¹)	Line shape	Peak Area*	Intensity ratio (I _D /I _G)
1.	Single-walled carbon nanotubes (SWNTs)	<i>D</i>	1330	90	Lorentzian	12158	0.17
2.	SWNTs	<i>G</i> ⁻	1501	40	Lorentzian	6032	0.17
3.	SWNTs	<i>G</i> ⁻	1523	16	Lorentzian	5152	0.17
4.	SWNTs	<i>G</i> ⁻	1543	20	Lorentzian	10242	0.17
5.	SWNTs	<i>G</i> ⁺	1590	30	Lorentzian	51176	0.17
6.	Carboxylated-SWNTs	<i>D</i>	1330	74	Lorentzian	19882	0.93
7.	Carboxylated-SWNTs	<i>G</i> ⁻	1512	46	Lorentzian	1513	0.93
8.	Carboxylated-SWNTs	<i>G</i> ⁻	1549	33	Lorentzian	4937	0.93
9.	Carboxylated-SWNTs	<i>G</i> ⁺	1589	27.4	Lorentzian	14847	0.93
10.	Carboxylated-SWNTs	<i>D</i> '	1612	22	Lorentzian	3460	

*Since we are interested in calculating I_D/I_G ratio and intensity axis is arbitrary unit, no unit is mentioned for the area.

The CoMoCat single-walled carbon nanotubes (SWNTs) used in the present investigation show characteristic radial breathing modes (RBM) in 125–250 cm⁻¹, *D*, *G* and *G*' band maxima at 1330, 1590 and 2618 cm⁻¹ respectively. Low I_D/I_G ratio (0.17) and high intensity of *G*' band shows high-quality SWNT bundles with uniform *sp*² walls.⁴ The *G* band splits into *G*⁺ and *G*⁻ corresponding to atomic displacements along tube axis and along the circumferential direction. The lower frequency of *G*⁻ mode is due to the curvature of the nanotube which softens the tangential vibration in the circumferential direction.⁵ The *G*⁻ mode is further deconvoluted into three modes corresponding to different Raman active modes. The carboxylic acid functionalization results in the formation of *sp*³ centers on the SWNT walls. The generated defect results in enhancement of I_D/I_G ratio to 0.93. The intensity of RBM and *G*' band decreases and additional feature at 1612 cm⁻¹ is *D*' band originating

from sp^3 defects on SWNT basal plane. These features are characteristic of functionalized SWNT with sp^3 centers on SWNT basal plane.^{3,6}

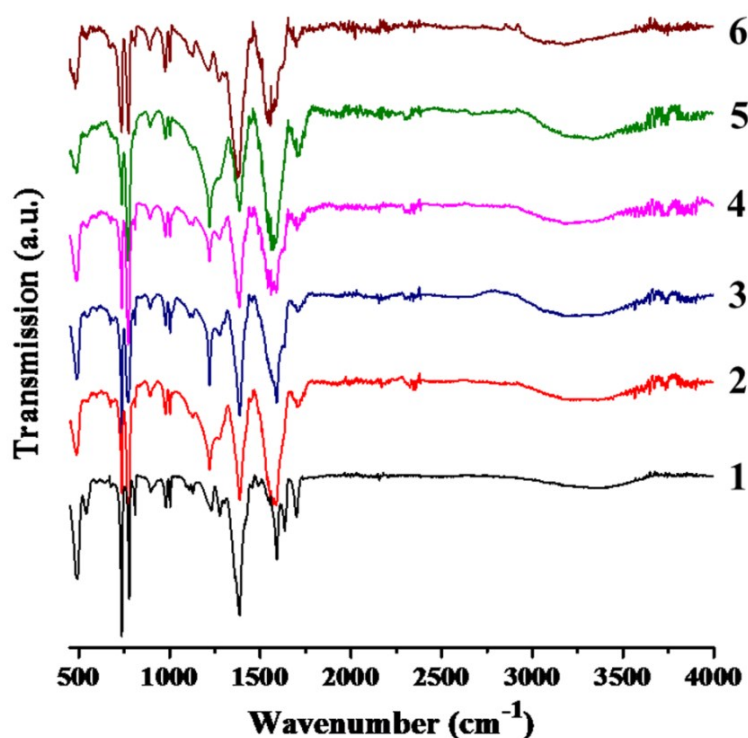


Fig. S4 Infrared spectra of (1) MOP, (2) MOPGr-1, (3) MOPGr-2, (4) MOPGr-3, (5) MOPNT-1 and (6) MOPNT-2.

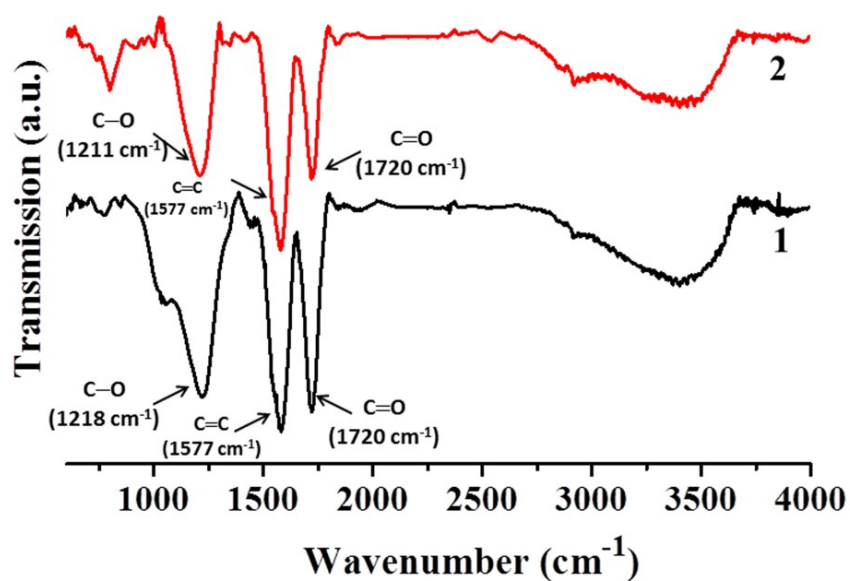


Fig. S5 Infrared spectra of (1) carboxylated-graphene and (2) carboxylated-SWNTs.

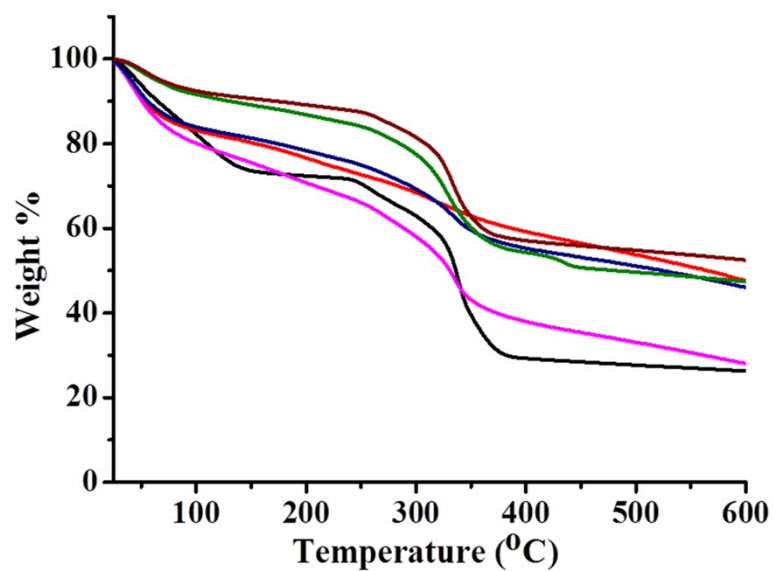


Fig. S6 Thermogravimetric analysis of MOP (black), MOPGr-1 (red), MOPGr-2 (blue), MOPGr-3 (magenta), MOPNT-1 (olive) and MOPNT-2 (wine).

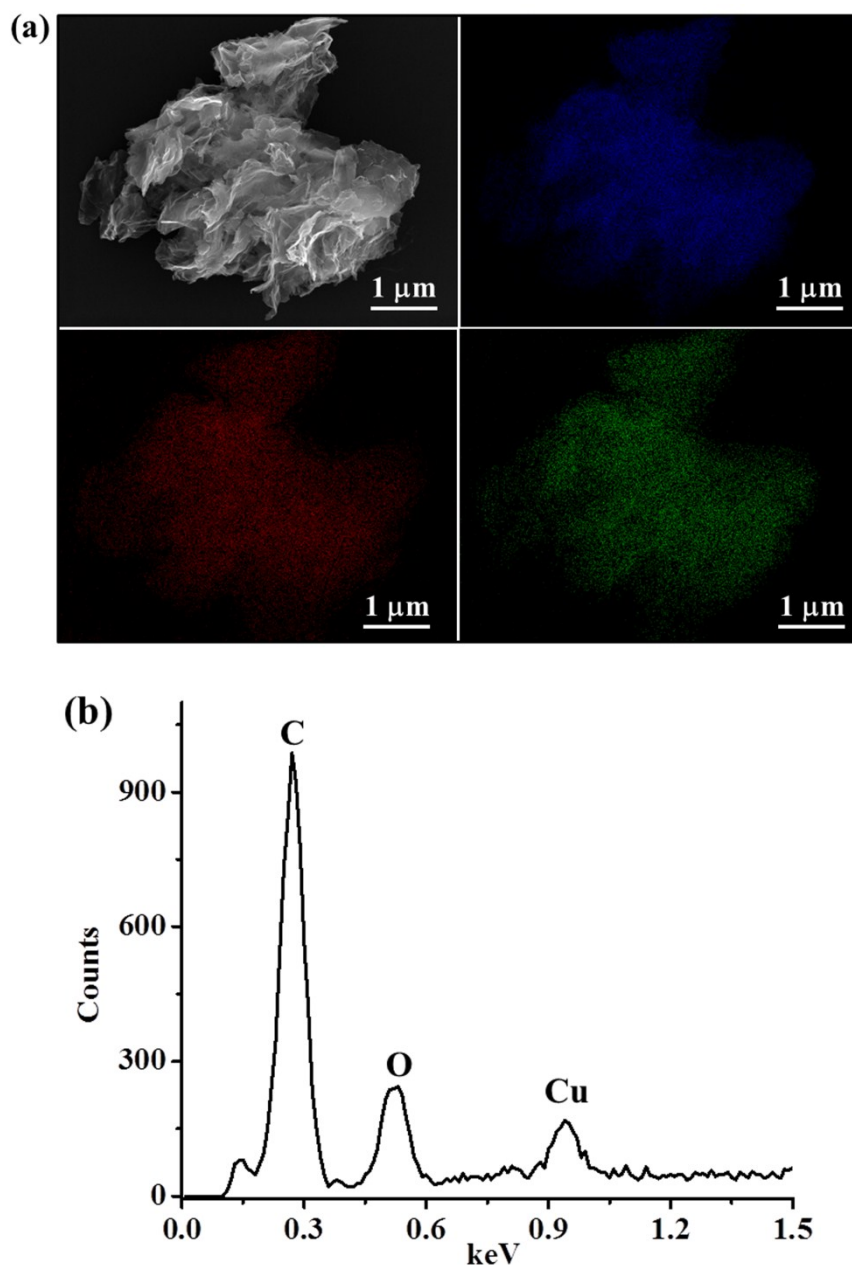


Fig. S7 (a) Scanning electron microscope image (SEM) and corresponding elemental mapping of MOPGr-1. The elemental mapping shows a uniform distribution of the constituent elements of metal-organic polyhedra C in blue, Cu in red, and O in green over the graphene basal plane. (b) Energy-dispersive X-ray spectroscopy (EDAX) of MOPGr-1 showing the presence of entire constituent elements of the hydroxylated metal-organic polyhedra (MOP) over the graphene basal plane.

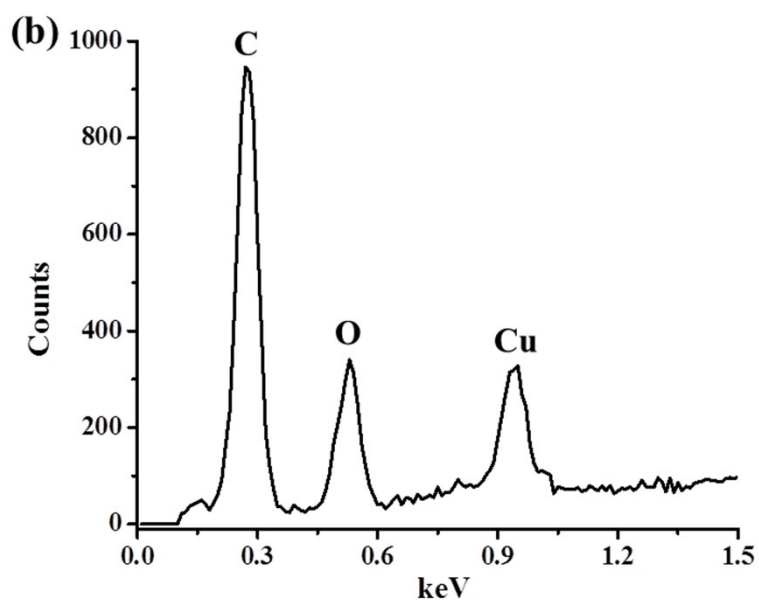
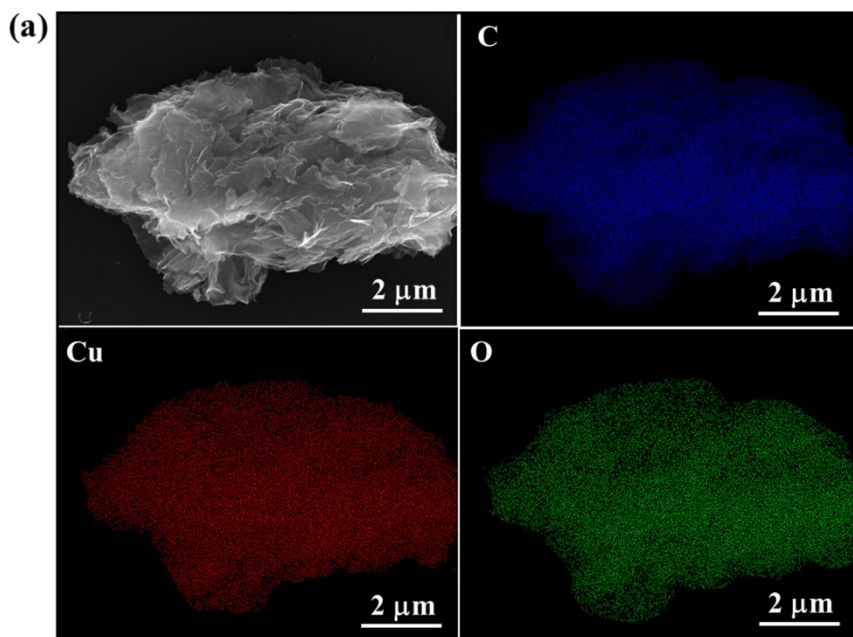


Fig. S8 (a) Scanning electron microscope image (SEM) and corresponding elemental mapping of MOPGr-3. The elemental mapping shows a uniform distribution of the constituent elements of metal-organic polyhedra C in blue, Cu in red, and O in green over the graphene basal plane. (b) Energy-dispersive X-ray spectroscopy (EDAX) of MOPGr-3 showing the presence of entire constituent elements of the hydroxylated metal-organic polyhedra over the graphene basal plane.

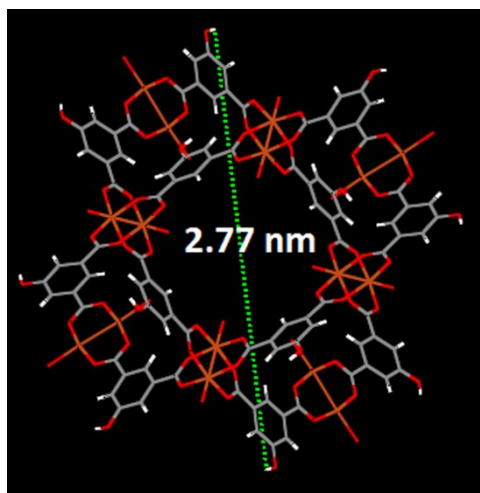


Fig. S9 Crystallographic external diameter of metal-organic polyhedra without external solvent molecules.

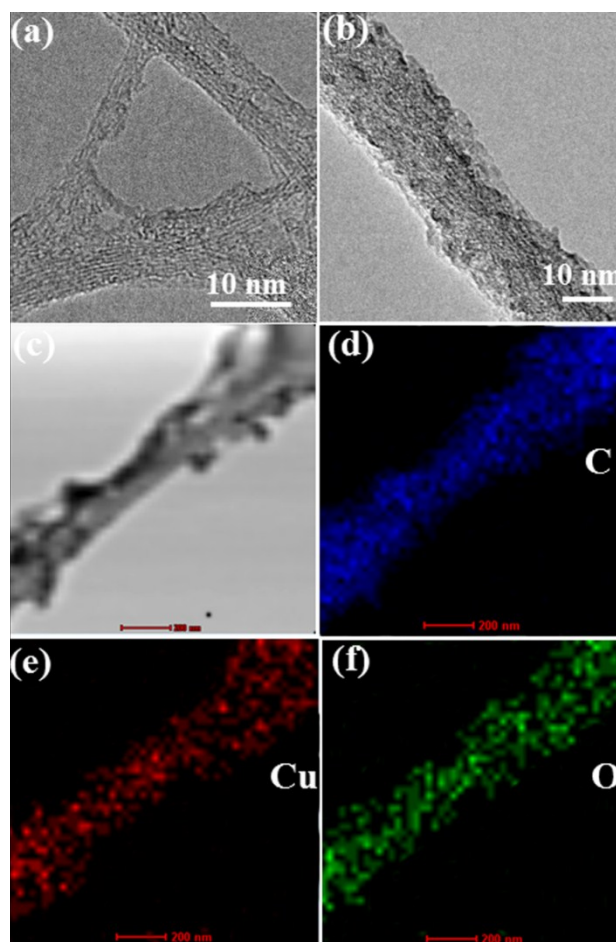


Fig. S10 Transmission electron microscope (TEM) images of (a) single-walled carbon nanotube (SWNT) bundles, (b) MOPNT-2 composite with uniformly distributed and intercalated MOP cages in SWNT bundle. (c, d, e and f) Annular dark-field scanning transmission electron microscopy (ADF-STEM) image of MOPNT-2 composite bundle and corresponding elemental mapping of the constituent elements C in blue, Cu in red and O in green. Scale bar corresponds to 200 nm.

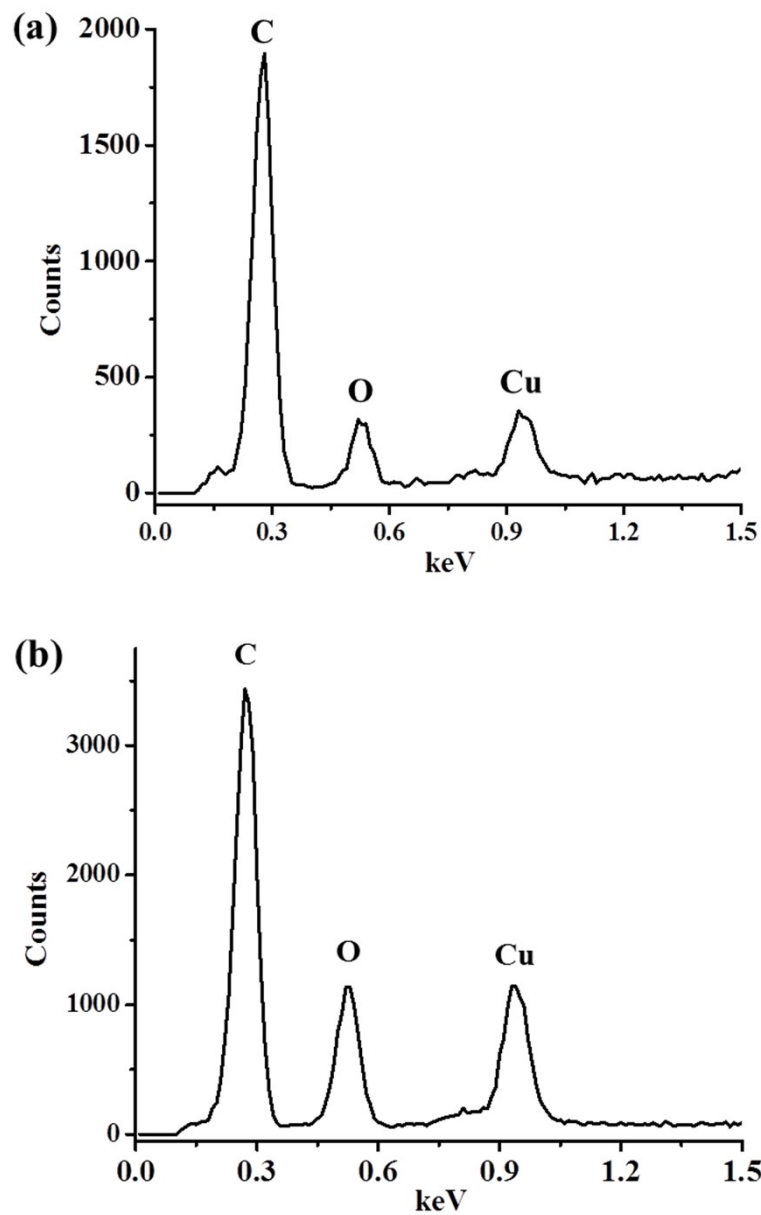


Fig. S11 Energy-dispersive X-ray spectroscopy (EDAX) of (a) MOPNT-1 and (b) MOPNT-2 showing the presence of entire constituent elements of the hydroxylated metal organic polyhedral over the single-walled carbon nanotube (SWNT) basal plane.

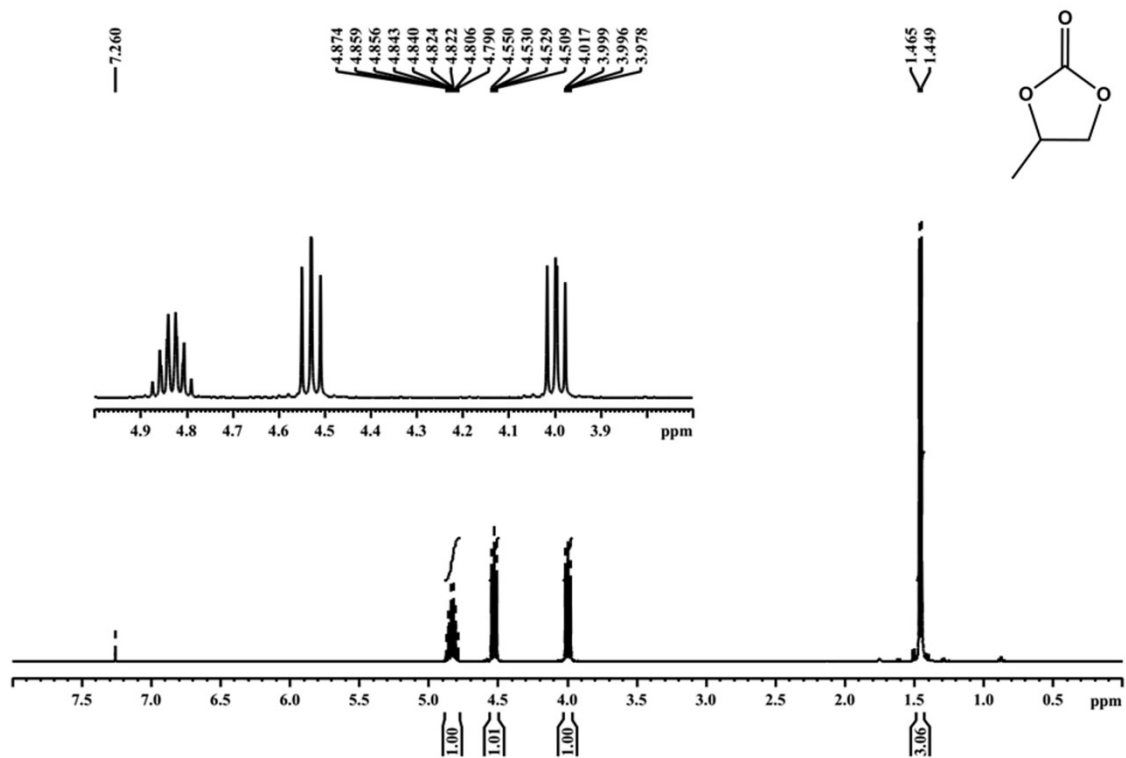


Fig. S12 Proton NMR spectrum of purified propylene carbonate from MOPGr-2 catalytic test run 1 obtained by vacuum distillation.

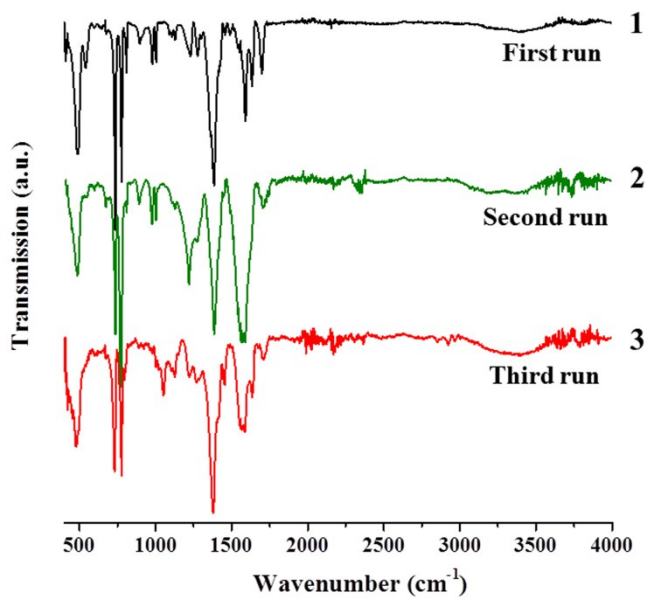


Fig. S13 Infrared spectra of MOPGr-2 catalyst after every catalytic test run.

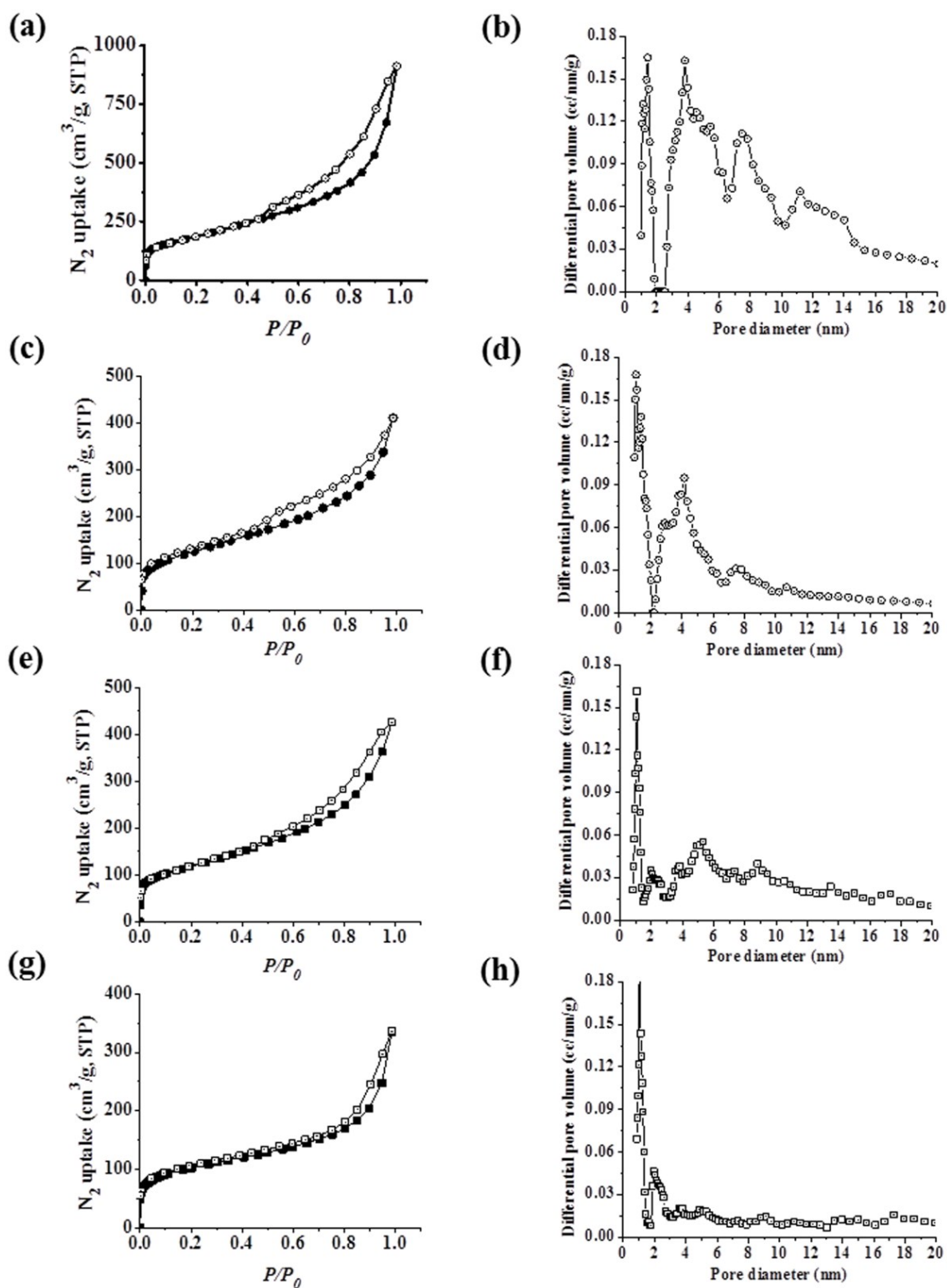


Fig. S14 Nitrogen adsorption–desorption isotherms and pore size distribution calculated using non-local density functional theory (NLDFT) calculation of (a, b) exfoliated-graphene (c, d) carboxylated–graphene, (e, f) single-walled carbon nanotubes (SWNTs) and (g, h) carboxylated-SWNTs at 77 K.

Table S3: Brunauer-Emmet-Teller (BET) surface areas and pore volume of different nanocarbons calculated using nitrogen adsorption isotherm.

Entry	Sample	BET Surface area (m ² /g)	(Pore volume, cm ³ g ⁻¹ at P/P ₀ ~ 1)
1	Exfoliated-graphene	654	1.4
2	Carboxylated-graphene	436	0.63
3	SWNTs	407	0.66
4	Carboxylated - SWNTs	353	0.52

The BET surface area of nanocarbon sample decreases on carboxylic acid functionalization due to decrease in the adsorbate accessible surface and agglomeration. Few-layer graphene obtained by thermal exfoliation of graphite oxide are less agglomerated in comparison to samples obtained by chemical reduction of graphite oxide. Exfoliated graphene (EG) has pore size distribution from microporous to mesoporous range and high surface area. High porosity makes exfoliated graphene a promising support material for catalyst design.

References:

- 1 R. Kumar, K. Jayaramulu, T. K. Maji and C. N. R. Rao, *Dalton Trans.*, 2014, **43**, 7383.
- 2 J.-R. Li and H.-C. Zhou, *Nat. Chem.*, 2010, **2**, 893.
- 3 M. A. Pimenta, G. Dresselhaus, M. S. Dresselhaus, L. G. Cancado, A. Jorio and R. Saito, *PCCP*, 2007, **9**, 1276.
- 4 A. Jorio, M. A. Pimenta, A. G. S. Filho, R. Saito, G. Dresselhaus and M. S. Dresselhaus, *New J. Phys.*, 2003, **5**, 139.
- 5 A. Jorio, R. Saito, G. Dresselhaus and M. S. Dresselhaus, *Phil. Trans. R. Soc. A*, 2004, **362**, 2311; (b) S. D. Mildred, *Phys. Scr.*, 2012, **2012**, 014002.
- 6 J. L. Hudson, M. J. Casavant and J. M. Tour, *J. Am. Chem. Soc.*, 2004, **126**, 11158; (b) C. A. Dyke and J. M. Tour, *Nano Lett.*, 2003, **3**, 1215.